This is the accepted manuscript made available via CHORUS. The article has been published as:

Pulsed Ion Beam Measurement of the Time Constant of Dynamic Annealing in Si

M. T. Myers, S. Charnvanichborikarn, L. Shao, and S. O. Kucheyev

Phys. Rev. Lett. **109**, 095502 — Published 27 August 2012

DOI: 10.1103/PhysRevLett.109.095502

Pulsed ion beam measurement of the time constant of dynamic annealing in Si

M. T. Myers,[1,2] S. Charnvanichborikarn,[1] L. Shao,[2] and S. O. Kucheyev[1]

[1]*Lawrence Livermore National Laboratory, Livermore, California 94550*

[2]*Department of Nuclear Engineering,*

Texas A&M University, College Station, Texas 77843

(Dated: July 18, 2012)

Abstract

Under ion irradiation, all crystalline materials display some degree of dynamic annealing when defects experience evolution after the thermalization of collision cascades. The exact time scales of such defect relaxation processes are, however, unknown even for Si at room temperature. Here, we use a pulsed ion beam method to measure a characteristic time constant of dominant dynamic annealing processes of about 6 ms in Si bombarded at room temperature with 500 keV Ar ions.

Bombardment with energetic ions inevitably produces lattice disorder in crystalline targets. An energetic ion propagating through a solid creates a collision cascade along its trajectory. The ballistic formation and thermalization of the cascade occur rapidly, at time scales of up to $\sim 10^{-12}$ s. Such regimes of cascade formation and thermalization (although challenging to access experimentally) are believed to be reasonably well understood.[1] In contrast, our current understanding of the evolution of defects after cascade thermalization, which is often referred to as *dynamic annealing* (DA), is limited for most materials.[1–4] Understanding mechanisms involved in DA is, however, highly desirable since DA plays a major role in the formation of stable post-irradiation disorder in most technologically relevant cases, including ion-beam-processing of semiconductors and radiation damage in nuclear materials.[2–6]

In this letter, we focus on the time scale of DA processes; i.e., a characteristic time constant τ over which the dominant processes of defect evolution persist after the thermalization of collision cascades. Such a time constant τ is determined by the thermal stability, effective diffusivity, and specific interaction processes of radiation-generated defects. Knowledge of τ is important for the development of physically sound models of damage accumulation in solids in order to control and fully exploit the effects of radiation damage. In particular, it is critical for extending laboratory findings to nuclear material lifetimes and dynamic regimes as well as to the time scales of geological storage of nuclear waste.[3,5,7]

Values of τ are, however, largely unknown even for arguably the best studied material system — single crystalline Si at room temperature (RT). Indeed, current estimates of τ for Si at RT range from $\sim 10^{-10}$ to $\gtrsim 10^{2}$ s,[8–13] inconsistency of 12 orders of magnitude! Such a large scatter in the estimates of τ is related to the fact that calculations and measurements of τ are not straightforward. Indeed, although molecular dynamics (MD) simulations are currently practical for following defect evolution only for $\lesssim 10^{-8}$ s, a number of MD studies by different groups[9–11] have suggested that defect evolution processes in Si at RT essentially cease for times $\gtrsim 10^{-10} - 10^{-9}$ s after cascade generation.

Other estimates of τ have involved an analysis of the dose rate effect (also often referred to as the flux effect); i.e., the dependence of ion-beam-produced stable lattice disorder on the dose rate when all the other experimental parameters are kept constant.[12–15] A dose rate effect is observed when defect stabilization time τ is comparable to the average time interval between the formation of spatially overlapping damage zones originating from

different collision cascades. Lateral dimensions of such damage zones are determined by both the average size of ballistic collision cascades and effective defect diffusion lengths, L_d. Hence, the dose rate effect combines both temporal (τ) and spatial (L_d) information that must be separated in order to obtain τ. Such estimates of L_d (and, hence, the extraction of τ from the experimental dose rate dependence of disorder) require serious assumptions about the explicit defect interaction processes.[12–14]

Spatial and temporal information can be separated in experiments with pulsed ion beams. Such a method was used by Linnros and co-workers,[16] who measured effective time constants of $\gtrsim$ 1 s for the process of ion-beam-induced epitaxial recrystallization of Si at elevated temperatures ($200-300$ °C). In this letter, we use a similar pulsed beam approach and find a characteristic DA time constant of $\sim$ 6 ms in Si bombarded at RT with 500 keV Ar ions.

Float-zone grown (100) Si single crystals (with a resistivity of about 5 Ω cm) were bombarded at RT with 500 keV $^{40}Ar^+$ ions at 7° off the [100] direction.[17] To improve thermal contact, samples were clamped to an Al holder with a thin layer of Cu-powder-impregnated thermal grease in between. To avoid complexity related to differences between instantaneous and average dose rates inherent to experiments with rastered ion beams, all irradiations were performed in a broad beam mode.[15,18] The central portion of the beam, estimated to be wider than $\sim$15 mm in diameter, was selected with a 4×5 mm^2 final beam defining aperture. A small sine ripple ($\sim$ 7 Hz) was applied to a set of electrostatic deflection plates in the horizontal direction to improve beam uniformity. This ripple extended the beam width by only $\sim$ 10% compared to the unperturbed beam. Beam pulsing was performed by applying high voltage pulses to a pair of plates deflecting the beam in the vertical direction off the final beam defining aperture.

After Ar ion irradiation, lattice disorder was measured by Rutherford backscattering/channeling (RBS/C) spectrometry with 2 MeV $^4He^+$ ions incident along the [100] direction and backscattered into a detector at 164° relative to the incident beam direction. All RBS/C spectra were analyzed with one of the conventional algorithms[19] for extracting the effective number of scattering centers (referred to below as "relative disorder").

Three sets of interrelated experiments were performed. First, we studied the damage buildup with a continuous beam with a constant dose rate and varied doses in the range of $(0.7-5.0) \times 10^{14}$ cm^{-2}. Based on the buildup curve measured, for further experiments, we selected a dose of 2.4×10^{14} cm^{-2} in a non-linear damage buildup regime where DA processes

are particularly pronounced.[15] A second set of experiments involved bombardment with a continuous beam to a dose of 2.4×10^{14} cm^{-2} with different dose rates. Third, we measured a dependence of lattice damage on the duration of the passive part of the ion beam cycle with all the other irradiation parameters kept constant.

Figure 1(a) shows selected depth profiles of lattice disorder for continuous beam irradiation to different doses with a constant dose rate of 1.2×10^{13} cm^{-2} s^{-1}. These depth profiles are bimodal, with the first peak reflecting the damage nucleated at or near the sample surface and the second broad bulk peak centered on a depth of ~ 450 nm, where the nuclear energy loss profile is maximum.[20] The bulk damage buildup with increasing ion dose, better illustrated in Fig. 2, is consistent with a number of previous systematic studies.[15,21,22] Disorder increases monotonically until full lattice amorphization is achieved. For doses of $\lesssim 1.4 \times 10^{14}$ cm^{-2}, damage accumulates close-to-linearly with dose. For larger doses, a super-linear increase in disorder is seen in Fig. 2. Such super-linearity has been attributed to critical energy density effects.[23] Dose rate effect studies of Titov and Carter[15] have shown that DA processes in Si are particularly pronounced in such a nonlinear regime. Hence, for the DA studies discussed below, we have selected a dose of 2.4×10^{14} cm^{-2} (marked by a star in Fig. 2).

Figure 1(b) shows selected depth profiles of disorder in Si irradiated with a continuous beam to a dose of 2.4×10^{14} cm^{-2} with different dose rates [in the range of $(0.1 - 10) \times 10^{12}$ cm^{-2} s^{-1}]. It is seen from Fig. 1(b) that lower dose rates result in less stable damage in the bulk peak region but a negligible effect on damage accumulation within ~ 40 nm from the sample surface. This observation is consistent with several previous reports.[15,24,25] It suggests different physical mechanisms of bulk and surface disordering.

Figure 1(c) shows depth profiles of disorder in Si irradiated with a pulsed beam when the total dose was split into a series of equal pulses. The inset in Fig. 1(c) shows a time dependence of the dose rate on the target and defines pulsed-beam-related parameters t_{on}, t_{off}, and F_{on}. For different curves shown in Fig. 1(c), all the irradiation parameters were kept constant (a dose of 2.4×10^{14} cm^{-2}, $t_{on} = 1$ ms, and $F_{on} = 1.2 \times 10^{13}$ cm^{-2} s^{-1}) except for t_{off}, the duration of the passive part of the ion beam cycle. Figure 1(c) reveals that the amount of stable disorder in the bulk decreases with increasing t_{off}, while surface damage is essentially independent of t_{off}.

Interestingly, for both pulsed beam irradiation [Fig. 1(c)] and continuous beam irradia-

tion with different dose rates [Fig. 1(b)], defect dynamics effects are evidenced only for the bulk and not the surface peak of disorder. This suggests that the same DA mechanisms are responsible for dose-rate and pulsed-beam effects. The similarity between pulsed irradiation and variable dose rate irradiation is further supported by Fig. 3, which compares the dependence of stable damage on the average dose rate [$F_{avg} = F_{on}/(1 + t_{off}/t_{on})$] for cases of pulsed and continuous beam irradiation.[26] Figure 3 shows that, for a given average dose rate, pulsed and continuous beam irradiation regimes create similar (although not identical) levels of stable disorder, supporting the above suggestion that the same DA processes are responsible for dose-rate and pulsed-beam effects.

As mentioned above, in contrast to the case of dose rate data, the DA time constant τ is clearly revealed in pulsed beam experiments. Figure 4 shows a trend of reduced bulk disorder with increasing t_{off}. An increase in t_{off} from 0 ms (i.e., a continuous beam) to 50 ms results in an $\sim 72\%$ decrease in bulk disorder. For $t_{off} \gtrsim 50$ ms, the disorder profile is essentially independent of t_{off} (within experimental errors), indicating that τ is on the order of magnitude of 10 ms.

The dependence of damage on t_{off} is related to the interaction of defects generated not only in different collision cascades but also by different pulses. As the beam is pulsed off the target, the defect concentration decreases via DA. For irradiation with $t_{off} >> \tau$, DA processes have essentially decayed in time intervals between individual ion pulses. This behavior can be treated phenomenologically in terms of competitive damage generation and annealing processes, as has been done by Carter[27] for a semi-quantitative description of the dose rate effect. Figure 4 suggests that defect evolution follows a second order behavior. Indeed, the dependence of the maximum defect concentration (n_{def}) obeys a second order kinetic equation ($\frac{\partial}{\partial t} n_{def} \propto n_{def}^2$):

$$n_{def}(t_{off}) = n_\infty + \frac{n_0 - n_\infty}{1 + \frac{t_{off}}{\tau}},$$

where n_0 and n_∞ are defect concentrations for $t_{off} = 0$ and ∞, respectively. A fit to the data in Fig. 4 with a nonlinear least-squares Marquardt-Levenberg algorithm yields $n_0 = 78$ at.%, $n_\infty = 17$ at.%, and $\tau = 6 \pm 1$ ms.[28] The DA efficiency, which we define here as $\frac{n_0 - n_\infty}{n_0}$, is $\sim 78\%$. Not surprisingly, a τ of 6 ms is in the range of previous estimates ($10^{-10} - 10^2$ s).[8–13] It is, however, two orders of magnitude smaller than the characteristic time constant of the

ion-beam-induced recrystallization process in Si at elevated temperatures studied by Linnros and co-workers.[16] This is consistent with an expectation that τ depends both on material properties and irradiation conditions (i.e., substrate temperature; ion dose; the maximum dose rate; and the average density of collision cascades,[29] determined by ion mass and energy). Future pulsed beam irradiation experiments should gain insight into how the DA time constant τ in Si depends on the type and concentration of dopants and on irradiation parameters. Data obtained with this method could also have important implications for the development of physically sound models of damage accumulation in solids. Clearly, a successful model for Si should include specific defect interaction processes with characteristic relaxation times and kinetics revealed by this work.

This pulsed-beam method could also be applied to study defect dynamics in technologically relevant materials other than Si. Of particular interest are material systems exposed to neutron irradiation. In such cases, understanding fundamental timescales of post-cascade-thermalization processes is crucial due to an inherent problem in the emulation of neutron and radioactive-decay-induced damage by ion irradiation, related to a large difference in rates of displacement generation between reactor operation or spent nuclear fuel storage conditions and ion irradiation experiments in the laboratory.

This work could be summarized as follows: (i) we have demonstrated an experimental pulsed ion beam method to measure characteristic time constants of DA processes in solids under irradiation, (ii) the DA time constant in Si at RT is $\sim$ 6 ms, (iii) the defect relaxation behavior measured for Si at RT suggests a second order kinetic process, and (iv) these results should stimulate future studies of dynamic defect interaction processes in other technologically relevant materials.

This work was performed under the auspices of the U.S. DOE by LLNL under Contract DE-AC52-07NA27344. L.S. thanks the support from NSF grant No. 0846835, and M.T.M. would like to acknowledge the LLNL Lawrence Scholar Program for funding. We are grateful to T. E. Felter for helpful discussions.

---

[1] See, for example, a review by M. T. Robinson, J. Nucl. Mater. **216**, 1 (1994); and references therein.

[2] J. S. Williams, Rep. Prog. Phys. **49**, 491 (1986).

[3] W. J. Weber, R. C. Ewing, C. R. A. Catlow, T. Diaz de la Rubia, L. W. Hobbs, C. Kinoshita, Hj. Matzke, A. T. Motta, M. Nastasi, E. K. H. Salje, E. R. Vance, and S. J. Zinkle, J. Mater. Res. **13**, 1434 (1998).

[4] See, for example, X.-M. Bai, A. F. Voter, R. G. Hoagland, M. Nastasi, and B. P. Uberuaga, Science **26**, 1631 (2010).

[5] Y. Guerin, G. S. Was, and S. J. Zinkle, MRS Bull. **34**, 10 (2009).

[6] H. M. Naguib and R. Kelly, Radiat. Eff. **25**, 1 (1975).

[7] N. M. Ghoniem, J. Nucl. Mater. **89**, 359 (1980).

[8] M.-O. Ruault, J. Chaumont, and H. Bernas, Nucl. Instrum. Methods **209/210**, 351 (1983).

[9] M.-J. Caturla, T. Díaz de la Rubia, L. A. Marqués, and G. H. Gilmer, Phys. Rev. B **54**, 16683 (1996).

[10] H. Hensel and H. M. Urbassek, Phys. Rev. B **57**, 4756 (1998).

[11] K. Nordlund, M. Ghaly, R. S. Averback, M. Caturla, T. Diaz de la Rubia, and J. Tarus, Phys. Rev. B **57**, 7556 (1998).

[12] M. Posselt, L. Bischoff, and J. Teichert, Appl. Phys. Lett. **79**, 1444 (2001).

[13] A. I. Titov, A. Yu. Azarov, L. M. Nikulina, and S. O. Kucheyev, Phys. Rev. B **73**, 064111 (2006).

[14] B.G. Svensson, C. Jagadish and J.S. Williams, Phys. Rev. Lett. **71**, 1860 (1993).

[15] A. I. Titov and G. Carter, Nucl. Instrum. Methods Phys. Res. B **119**, 491 (1996).

[16] J. Linnros and G. Holmén, J. Appl. Phys. **62**, 4737 (1987); J. Linnros, W. L. Brown, and R. G. Elliman, Mater. Res. Symp. Proc. **100**, 369 (1988).

[17] The 4 MV ion accelerator (National Electrostatics Corporation, model 4UH) at Lawrence Livermore National Laboratory was used for both ion irradiation and ion beam analysis.

[18] P. J. Schultz, C. Jagadish, M. C. Ridgway, R. G. Elliman, and J. S. Williams, Phys. Rev. B **44**, 9118 (1991).

[19] K. Schmid, Radiat. Eff. **17**, 201 (1973).

[20] J. Ziegler, J. Biersack, and U. Littmark, The Stopping and Range of Ions in Solids, Vol. 1 (Pergamon, New York, 1985).

[21] G. Bai and M.-A. Nicolet, J. Appl. Phys. **70**, 3551 (1991).

[22] E. C. Baranova, V. M. Gusev, W. V. Martynenko, C. V. Starinin, and I. B. Haibullin, Radiat.

Eff. **18**, 21 (1973).

[23] M. L. Swanson, J. R. Parsons, and C. W. Hoelke, Radiat. Eff. **9**, 249 (1971).

[24] S. A. R. Al-Hashmi and G. Carter, Radiat. Eff. **102**, 83 (1987).

[25] A. I. Titov, V. S. Belyakov, and A. Yu. Azarov, Nucl. Instrum. Methods Phys. Res. B **212**, 169 (2003).

[26] Note that the average dose rate is not conserved in experiments with variable t_{off} and constant t_{on} and F_{on}.

[27] G. Carter, J. Appl. Phys. **79**, 8285 (1996); and references therein.

[28] Attempts to fit the data shown in Fig. 4 with a single exponential decay curve (i.e., the solution of the first order kinetic equation) have resulted in an inferior fit compared to the case of fitting with the solution of the second order kinetic equation discussed in the text. However, even such a single exponential decay fit, albeit poor, yields $\tau = 7 \pm 2$ ms, demonstrating that the value of τ measured with the pulsed beam method is weakly dependent on the particular model of defect interaction processes assumed.

[29] See, for example, S. O. Kucheyev, A. Yu. Azarov, A. I. Titov, P. A. Karaseov, and T. M. Kuchumova, J. Phys. D: Appl. Phys. **42**, 085309 (2009); and references therein.

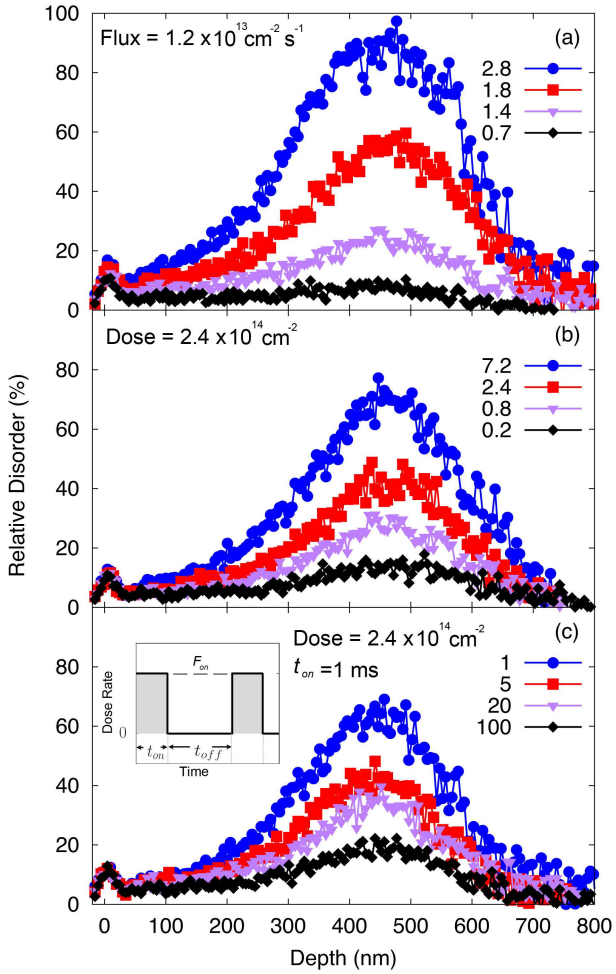

FIG. 1. (Color online) Selected depth profiles of relative disorder in Si bombarded at RT by 500 keV Ar ions (a) with a continuous beam with a constant dose rate of 1.2×10^{13} cm^{-2} s^{-1} to various doses (given in the legend in units of 10^{14} cm^{-2}), (b) with a continuous beam to the same dose of 2.4×10^{14} cm^{-2} with different dose rates (given in the legend in units of 10^{12} cm^{-2} s^{-1}), and (c) with a pulsed beam with different values of t_{off} (given in the legend in units of 10^{-3} s) and all the other parameters fixed (dose $= 2.4 \times 10^{14}$ cm^{-2}, $t_{on} = 1$ ms, and $F_{on} = 1.2 \times 10^{13}$ cm^{-2} s^{-1}). The inset in (c) shows a schematic of the time dependence of the dose rate for pulsed beam irradiation, defining t_{on}, t_{off}, and F_{on}.

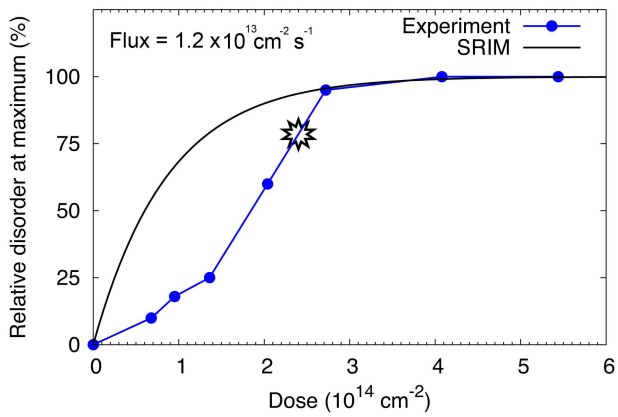

FIG. 2. (Color online) Dose dependence of relative disorder at the maximum of the bulk defect peak for Si bombarded at RT by 500 keV Ar ions with a dose rate of 1.2×10^{13} cm^{-2} s^{-1} [based on ion channeling data such as shown in Fig. 1(a)]. The dash line shows a SRIM-code-predicted[20] dependence, taking into account damage saturation upon amorphization. The star denotes the dose used in studies of defect dynamics.

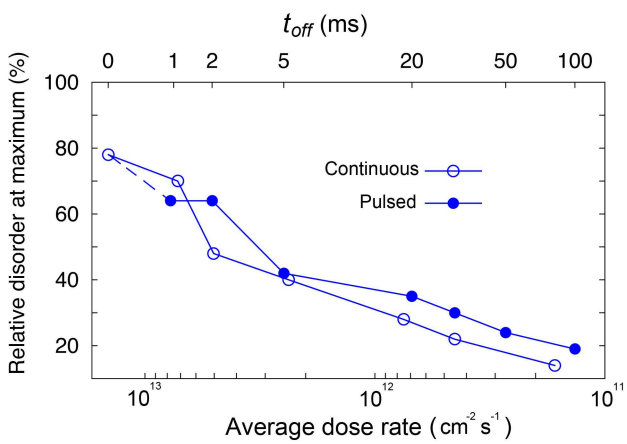

FIG. 3. (Color online) Dependence of relative disorder at the maximum of the bulk defect peak on the average dose rate, F_{avg} (for both continuous and pulsed beam irradiation) [bottom axis] and on t_{off} (for pulsed beam irradiation) [top axis] for Si bombarded at RT by 500 keV Ar ions to a dose of 2.4×10^{14} cm^{-2}. For pulsed experiments, the maximum dose rate was 1.2×10^{13} cm^{-2} s^{-1} and t_{on} [defined in the inset of Fig. 1(c)] was 1 ms.

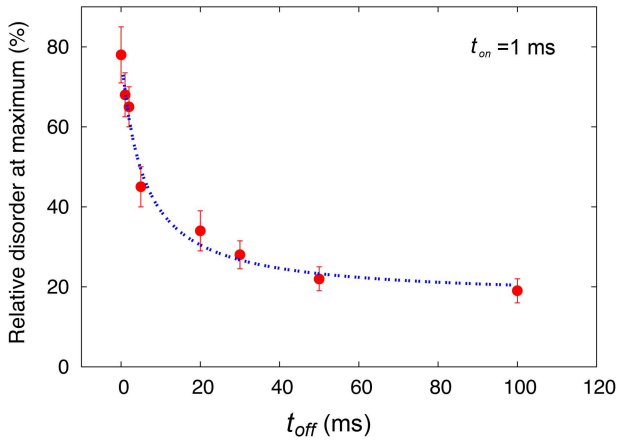

FIG. 4. (Color online) Dependence of relative disorder at the maximum of the bulk defect peak on the passive portion of the beam t_{off}, with a fitting curve of the second order rate equation, discussed in the text, shown by a dash line. Error bars correspond to peak-to-peak noise in RBS/C-derived disorder profiles such as shown in Fig. 1(c).